CODING EFFICIENCY OF INNER HAIR CELLS
AT THE THRESHOLD OF HEARING

Ilse C. Gebeshuber[1] and Frank Rattay[2]

[1]*Institut für Allgemeine Physik and* [2]*TU-BioMed*
University of Technology, Vienna
Wiedner Hauptstraße 8-10/1145
A-1040 Wien, Austria

1.   Introduction

The human hearing threshold curve for pure tones is a nonlinear function of frequency (Figure 1). The minimum sound pressure required for an audible sensation to occur is frequency dependent and spans approximately five orders of magnitude. In the highly sensitive region of the spectrum between 2 and 5 kHz an intensity as low as 10^{-12} W/m^2 is sufficient to evoke an audible sensation.

The current modeling study investigates the efficiency with which the mechanical stage of transduction in the inner ear is transformed into a neural form (i.e., mechano–electric transduction) for low-intensity sinusoidal signals across a range of frequencies. Our goal is to gain insight into the basic physiological properties that underlie the human hearing threshold curve.

The inner hair cells (Figure 2) play a key role in mechano-electric transduction. In the human inner ear are three rows of outer hair cells (OHCs) and one row of inner hair cells (IHCs). A primary function of the OHCs is to amplify the magnitude of low-intensity signals [1][16][24]. IHCs serve as the primary (if not the sole) conduit of frequency-selective information to the brain via their innervation of the auditory nerve. Deflection of the hair cell stereocilia modulates the probability of the cell's transduction channels opening and closing and is responsible for the voltage fluctuations observed within the cell. Such fluctuations provide a low-pass filtered "image" of the stereociliary displacement (along with additional stochastic components resulting from channel gating). In the "active" zones, at the base of the cell, sufficient depolarization of the receptor potential results in Ca^{2+}-induced neurotransmitter release. This transmitter release, if of sufficient magnitude, results in depolarization of proximal auditory-nerve fibers, resulting in the generation of action potentials that are propagated into the auditory brainstem.

The transduction mechanism is so sensitive that displacements resulting from stereociliary Brownian motion contribute significantly to the spontaneous discharge activity observed in highly sensitive (i.e., high spontaneous rate) auditory-nerve fibers [8][10][31]. Acoustically generated displacements less than the thermal motion of the stereocilia are sufficient to cause an audible sensation. The Brownian motion in this instance enhances the detection of weak signals via a mechanism known as "stochastic resonance" [9][10][31]. Stochastic resonance is based on nonlinear statistical dynamics through which information flow in a multistate system (such as the transduction channel of the inner hair cell or the all-or-none process of spike generation) is enhanced by the presence of optimized random noise [23].
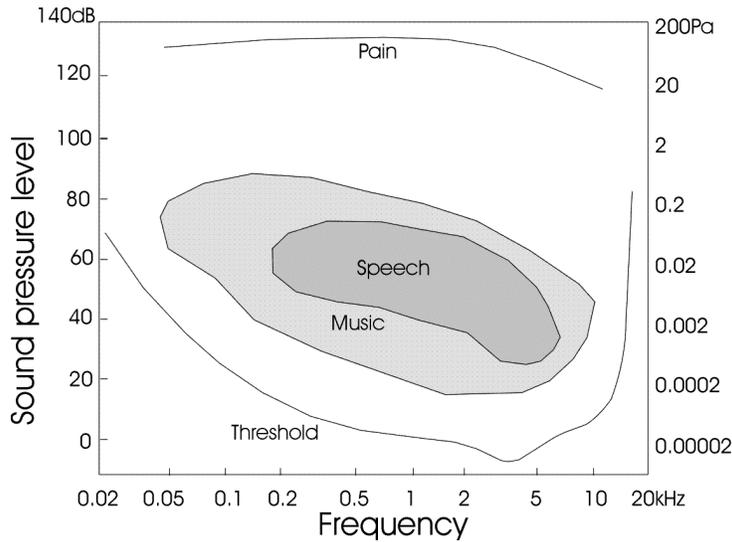
Figure 1 Region of human audibility (i.e., the range between the threshold of hearing and of pain). The intensity is scaled in dB, while the sound pressure is shown in Pascals. Note that the range of pressure variation covers 7 orders of magnitude. Adapted from [33].

Figure 3 shows the number of auditory-nerve fibers innervating an "average" IHC of a normal human cochlea. The innervation density varies as a function of cochlear-frequency position in a manner comparable to the hearing threshold curve (Figure 1). In the mid-frequency region the innervation density reaches a maximum of ca. 15 fibers per IHC. About sixty percent of these fibers are highly sensitive and exhibit relatively high rates of spontaneous activity (18–120 spikes/s).

The highly sensitive nerve fibers change their spiking patterns for low- and mid-frequency signals close to the threshold of hearing as follows: the first sign of influence on the firing of many spontaneously active fibers by a pure tone is phase-locking of the spikes [28] [29]. This may occur at an intensity far below that required to evoke an increase in mean firing rate [12]. This phase-locking effect does not occur for high-frequency signals as a consequence of the jitter associated with interspike times. Afferent fibers may respond differently each time a stimulus of a given amplitude is presented since fluctuations in excitability and latency are directly associated with fluctuations in the membrane resting potential [3].

Endogenous noise in the resting neural membrane potential of nerve fibers decreases with increasing diameter. The noise is on the order of 1 mV root-mean-square (r.m.s.) for myelinated fibers of small diameter and less than 1 mV for larger-diameter myelinated fibers [4]. The mean inner diameter of central axons of human auditory-nerve fibers has an unimodal distribution and ranges between 2.7 and 3.1 μm (with the exception of smaller fibers at the base of the cochlea) [30].
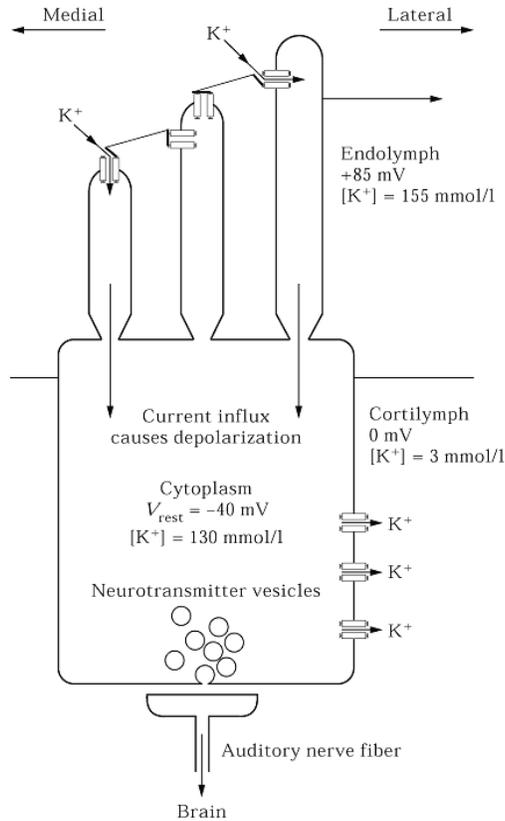
Figure 2 Schematic illustration of an inner hair cell. Endolymphatic fluid motion caused by the movement of the middle ear ossicles induces displacement of the stereocilia of the auditory receptor cell. The stereocilia of an inner hair cell are interconnected by links (elastic protein filaments). The open-close kinetics of transduction channels located close to the top of each stereocilium depend on stereociliary deflection (Figure 4). Even in the resting state the transduction channel open probability is about 15%. Due to potential gradients, ion currents (mainly potassium) enter the cell through the transduction channels and leave through ion channels in the cell body membrane, resulting in a resting potential of ca. –40 mV in the unstimulated hair cell and potential changes of several mV following stereociliary displacement. A potential change as low as 0.1 mV may cause neurotransmitter release and thereby evoke a spike in an auditory-nerve fiber. Note the tapering of the bottom portion of the stereocilia endings. In humans the inner hair cell stereocilia are arranged in a 20 by 3 matrix, with 20 short, 20 intermediate-length and 20 long elements. Each stereocilium behaves like a rigid rod pivoting around its insertion point into the cuticular plate.

2. Materials and Methods

2.1 Brownian Motion

The IHC stereocilia are interconnected by tip-links and horizontal links, and act like stiff rods capable of pivoting around their insertion point into the cuticular plate (Figure 2). The Brownian motion of the stereociliary tips is calculated using a reduced version of the stereocilia linear chain model [31]. The r.m.s. value of the modeled intrinsic bundle noise is ca. 2 nm, which is in accordance with experimental data [2]. The small amplitude of the fluctua-
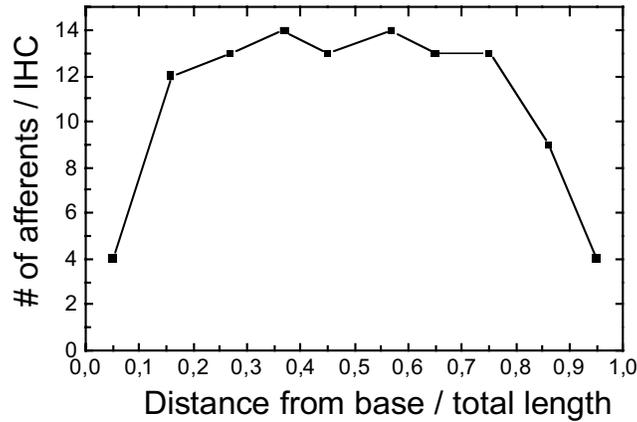
Figure 3   Innervation density per inner hair cell in a normal human cochlea (adapted from [7]). Sixty percent of the afferent nerve fibers are highly sensitive. The transformation from normalized distance, d, to the characteristic frequency, f, of the nerve fiber obeys the following relation in the human: $f=200(10^{2d}-0.7)$ [13].

tions due to Brownian motion can be appreciated by comparing them to the dimensions of a single stereocilium (ca. 0.2 μm in diameter) or to the bundle's displacement-response relationship (Figure 4). In vestibular hair cells of the frog, viscous drag acting on the bundle limits Brownian motion to relatively low frequencies (200–800 Hz) [2]. However, theoretical considerations suggest a corner frequency of ca. 4 kHz for thermal fluctuations in mammalian hair cells [31], which implies that stochastic resonance may also be effective in the mid-frequency range of audition.

The overall displacement of the hair bundle in response to low-intensity signals is the sum of the bundle movements resulting from Brownian motion as well as from the signal-induced displacement. The signal-to-noise ratio is defined as the ratio of the r.m.s. magnitude of the signal and the r.m.s. level of the stereociliary deflections attributable to Brownian motion. Our
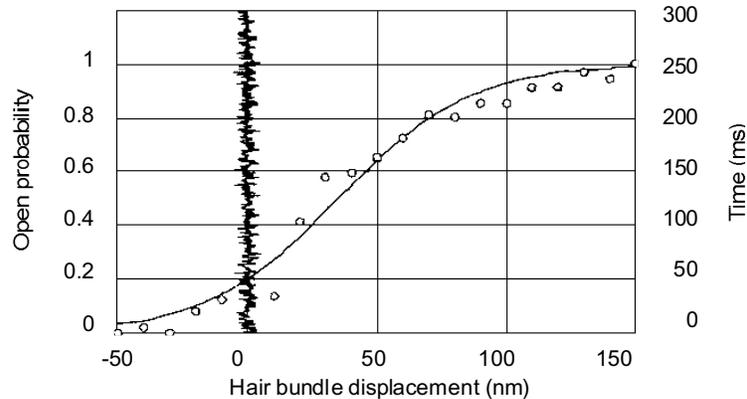
Figure 4   The relation of a 300-ms trace of simulated Brownian motion (low-pass filtered, 2 nm r.m.s. white noise) to a cell's displacement-response behavior. This function relates the probability of transduction channels being open (left y-axis) to the hair bundle displacement (x-axis). Note that in this specific case the transduction-channel, resting-open probability is 0.2. Adapted from [18].
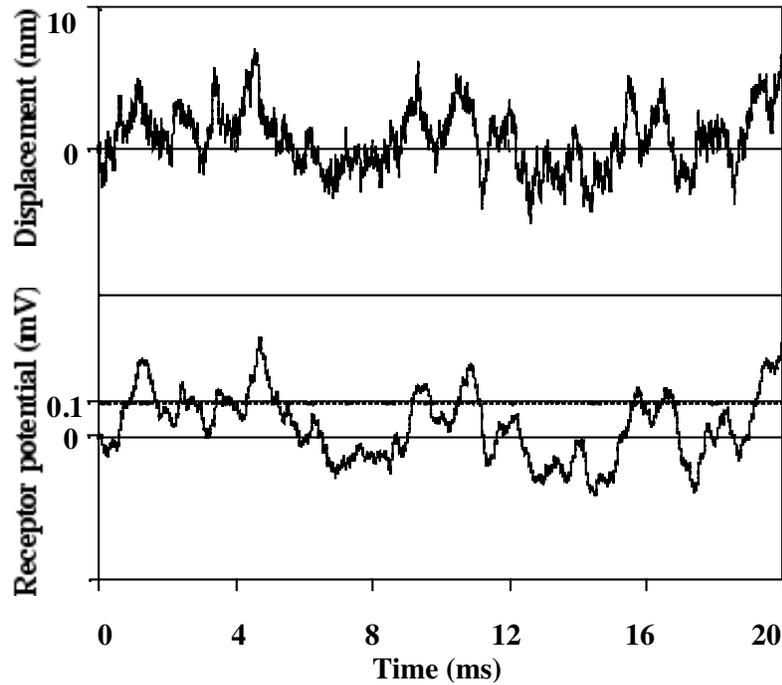
Figure 5 Modeled mechanical and electrical fluctuations due to Brownian motion: the intracellular receptor potential changes (bottom trace) are a low-pass filtered version of stereociliary displacements (top trace) with an additional amount of noise resulting from transduction channel kinetics.

simulation investigates the effects of signal-to-noise ratio (whose normalized range is between 0 and 1 — equivalent to stimulation of the hair bundle with an amplitude between 0 and 2.12 nm r.m.s.). The frequency of the stimulating, deterministic signals ranges between 0.2 and 20 kHz. Figure 5 shows a 20-ms time series of hair-bundle displacements resulting from Brownian motion.

2.2 Endogenous Transduction Channel Noise

The receptor potential fluctuations in the IHC are calculated using a model for the mechano–electrical transduction in inner hair cells [25]. The model uses equivalent electric circuits for cell membrane and cytoplasm (i.e., RC components and batteries). The kinetics of the transduction channels are modeled as Markov processes without memory: whether the channel stays open or closed depends only on its current open probability and not on the length of time the channel has already been open or closed.

For displacements in the range of a few nm, the relation between the stereociliary displacement and the open probability of the transduction channels is linear (Figure 4) [22]. For zero displacement the open probability of the transduction channel is about 0.15. For small displacements to the lateral side the transduction channel open probability increases, resulting in an influx of potassium ions. This influx causes a depolarization of the receptor potential from its resting state (ca. –40 mV). Displacement to the medial side decreases the open probability, resulting in fewer potassium ions entering the cell and a concomitant hyperpolarization of the membrane potential. Since the model's inner-hair-cell membrane time constant, τ, equals 0.255 ms [25], the IHC potential can be thought of as a low-pass-filtered version of the stereociliary displacement pattern combined with additional noise resulting from the stochastic components in channel gating (Figure 5).
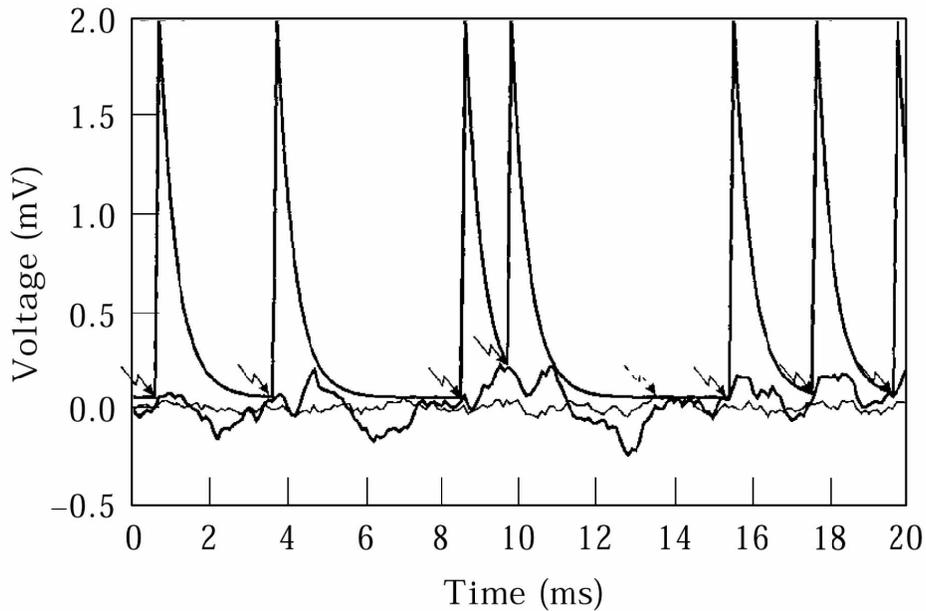
Figure 6   Simulated receptor potential changes and resulting firing behavior. The noise in the voltage fluctuations evoked by a weak 500-Hz signal alone (thin line, hypothetical case without Brownian motion) is a consequence of the endogenous transduction channel noise. Only in one instance (marked by a dashed arrow at 13.5 ms) are the fluctuations large enough to reach the threshold of spiking at 0.1 mV. The compound fluctuations caused by the same sinusoidal signal, the endogenous transduction channel noise and the thermal fluctuations with a signal-to-noise ratio of 0.2 show the enhancing effect of the noise: Seven spikes may occur within 20 ms among associated auditory-nerve fibers. The recovery behavior after spiking is modeled by an exponential decay of the threshold curve. As soon as the voltage fluctuations exceed threshold a new spike can occur.

2.3 Jitter in the Spiking Times: Refractory Period

The spike-generation process is modeled in the following way. Whenever the voltage fluctuations of the IHC exceed a threshold of 0.1 mV (a value sufficient for neurotransmitter release in hair cells [15]), a spike may be generated in an afferent fiber. Because of the stochastic nature of spike generation the probability for spiking is adjusted to obtain a mean spontaneous discharge rate of ca. 100 spikes/s in the resting state [27]. Jitter in the firing pattern is modeled by a single-sided, normally distributed time shift whose standard deviation is 50 μs. Since the absolute refractory period of an auditory-nerve fiber is ca. 0.8 ms (in the cat [19]), the time constant of the exponentially decaying threshold curve is set to 0.25 ms and the maximum value for the height is set to 2 mV (Figure 6).

The spike rate associated with a just-supra-threshold signal does not exceed the spontaneous rate of 100 spikes/s. However, nerve impulses become increasingly phase-locked to the acoustic signal as the signal level increases [10][11][12][14][28][29].
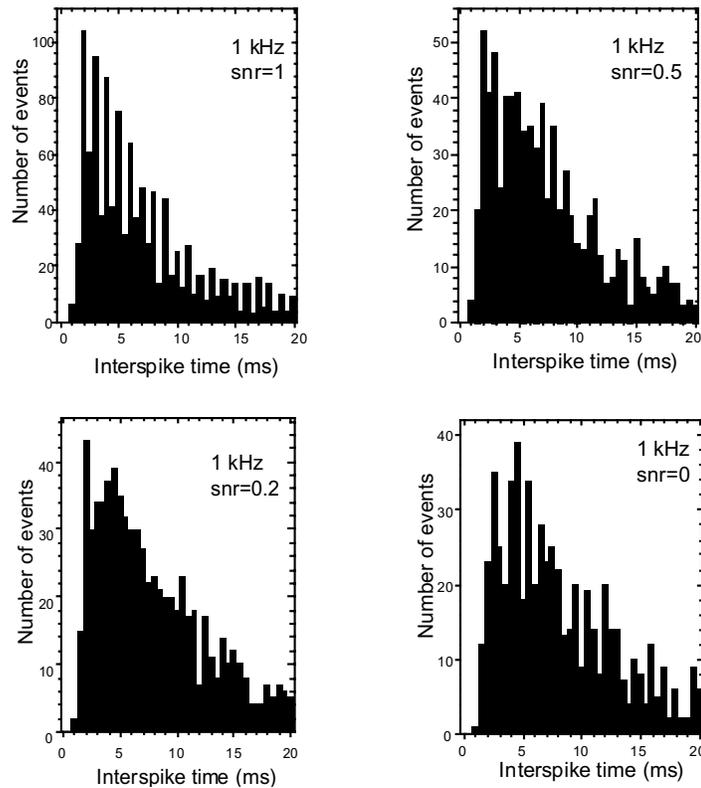
Figure 7 ISIHs for a 1-kHz signal at several signal-to-noise ratios. With increasing SNR, the proportion of spikes in a specific half of the signal period increases relative to the other half. Signal duration is 1s. The model's output represents the activity of 12 highly sensitive nerve fibers. Histogram binwidth is 0.5 ms.

3. Results

In this section we present an analysis of the frequency information encoded in the interspike interval histograms (ISIHs) of simulated auditory-nerve firing patterns induced by low-intensity, sinusoidal hair bundle deflections.

When the histogram binwidth is precisely half the period of the stimulating signal, phase-locking of the interspike times can be readily observed in the ISIHs as an up-down-up-down pattern. The distribution of spikes is non-uniform across time, being concentrated in a restricted portion of the stimulus cycle. This phase-locked behavior is manifested in the interspike interval histogram in the form of modes associated with intervals that are integral multiples of the stimulus period. The maximum interspike time considered in our model is 20 ms. Figure 7 shows ISIHs for stereociliary displacements at 1 kHz. With increasing SNR, the spikes tend to occur increasingly in the first half of the stimulus period (i.e., the phase-locking effect becomes increasingly apparent). A means to assess the information contained in the ISIH is to measure the ratio of spikes occurring during the positive half-wave of the stimulating signal relative to the total number of spikes. This ratio is a measure of the proportion of informative spikes, and has been used as a metric of phase-locking performance [28].

With decreasing signal frequency the number of bins (and therefore the fine structure information) associated with the ISIH decreases (Figure 8). Although the number of infor-
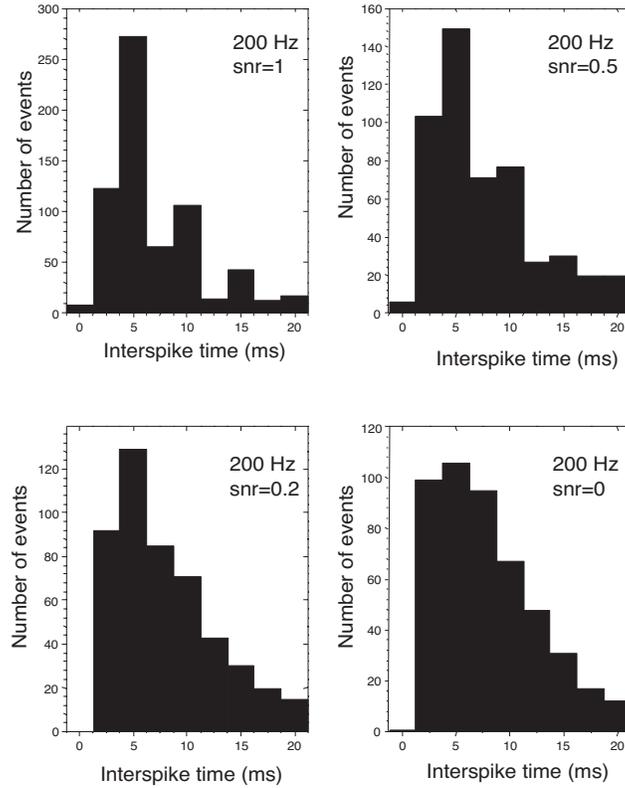
Figure 8 ISIHs for a 200-Hz signal at several signal-to-noise ratios. Signal presentation time is 1s. 5 highly sensitive nerve fibers, binwidth is 2.5 ms.

mative spikes is still greater than 50% for a 200-Hz signal with an SNR of 0.2, the number of events in each bin tend to decrease exponentially as occurs when the SNR is 0. The fine structure in the histogram, with valleys associated with integral multiples of the negative half-wave of the stimulating signal, is lost.

In a previous study we had analyzed the information contained in the ISIHs with artificial neural networks [9] [26]. In the mid-frequency range the neural net accurately detected the signal more than 75% of the time for signal-to-noise ratios as low as 0.1. Taking into consideration the parallel information transfer from several IHCs to the central nervous system considerably reduces the signal duration required to accurately detect the presence of a signal.

The information contained in the ISIHs is evaluated by calculating the number of informative spikes over a range of frequencies and signal-to-noise ratios. The resulting frequency-response-efficiency tuning curves are illustrated in Figure 9. The curves for low SNRs may be thought of as analogous to human hearing threshold curves for pure tones, as they reflect the combined effects of stereociliary Brownian motion, endogenous hair cell noise, the stochastic nature of neurotransmitter release and the innervation density of primary auditory afferents in various frequency bands. Note that this simulation study models threshold curves as they are reflected in the transduction of small sinusoidal displacements of the stereocilia. Furthermore, any possible effect of inhibitory efferent innervation of afferent nerve fibers (see e.g. [5] [6]) on the spiking pattern is neglected due to an absence of experimental data.
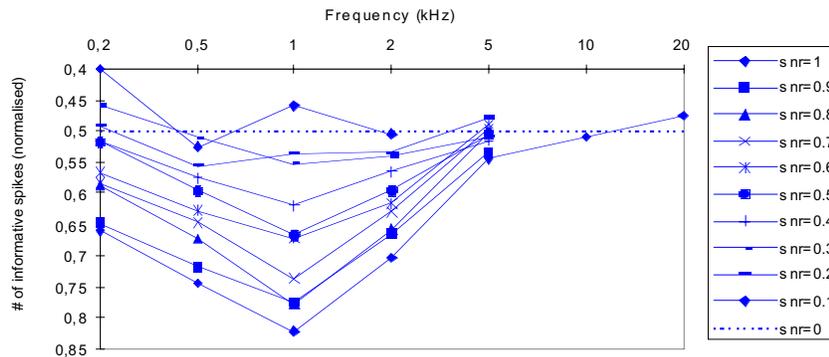
Figure 9 Frequency-response efficiency tuning curves for a multicellular model of peripheral auditory coding, (i.e. normalized number of informative spikes for several frequencies and signal-to-noise ratios). For an SNR of 0 there is no signal present and half of the spikes are phase-locked at chance level (i.e. the normalized number of informative spikes is 0.5). For frequencies between 0.2 kHz and 2 kHz, the phase-locking effect increases with increasing SNR (i.e., the normalized number of informative spikes increases well above 0.5). In the 5 kHz case there is virtually no apparent phase-locking. The 10 kHz and 20 kHz cases show no effect of phase-locking at all. In such instances only the normalized number of informative spikes for an SNR of 1 is presented. For high signal-to-noise ratios the curves are V-shaped. When the signal is reduced in amplitude and the influence of noise increases, the curves broaden and eventually invert at 1 kHz. Stimulus duration for each data point is 1s. For information concerning frequency-dependent innervation density cf. Figure 3.

At 1 kHz (the frequency which can be encoded and decoded optimally under the present conditions) a reversal of the shape of the curve appears at very low signal-to-noise ratios. When the signal level increases, the curves invert and become sharper. This effect corresponds to experimental results observed in noise-induced tuning-curve changes in mechanoreceptors of the rat foot [17]. Modeling the transduction channel kinetics as a Markov process results in a frequency-dependent peak-to-peak receptor potential. For low and high frequencies, the sub-threshold deterministic stimuli elicit voltage changes further from threshold than ones evoked by mid-frequency stimuli. Therefore, the optimal noise level is also frequency-dependent and the inversion of the tuning curve for low SNR stimuli is directly related to the threshold shift (cf. Figure 9 in [17]).

The 2-kHz case is comparable to the 1-kHz case. Increasing the SNR increases the number of informative spikes from approximately (but just higher than) chance level for an SNR of 0.1 to over 70% for an SNR of 1.

For high-frequency signals the jitter in the nerve firing pattern destroys the fine structure in the ISIH. However, statistics of the discharge pattern over a longer period would still contain some temporal information germane to 5 kHz, at least for signal-to-noise ratios close to one. For signals in the range of 10–20 kHz, increasing the signal does not further increase the number of informative spikes since the jitter completely destroys the phase-locking information. Therefore, the psychophysical hearing threshold data for the high-frequency portion of the spectrum cannot be attributed to phase-locking. This means that for high-frequency signals frequency information must be coded in a different way. The increase in spike rate is the most likely candidate for providing this information.

4.　Discussion

In this study we have shown that a compound model of coding efficiency of inner hair cells at the threshold of hearing accounts for certain properties of the psychophysically measured human hearing threshold curve (Figure 1). Through the mechanism of stochastic resonance the Brownian motion of IHC stereocilia makes otherwise undetectable low-intensity signals audible. The jitter in auditory-nerve fiber spike times accounts for the steep slope in the threshold curve at high frequencies. In the low-frequency portion of the spectrum the long interspike times prevent detection of the signal, especially at low signal-to-noise ratios.

Changes in hair-bundle morphology also affect the pattern of thermal fluctuations of the stereocilia and therefore exert some influence on spontaneous activity in auditory-nerve fibers. In milder instances of acoustic trauma, morphological changes are only found in the rootlets of the stereocilia (which appear less dense in electron micrographs) [21]. In more severe instances of trauma (typically resulting in permanent damage) kinks or fractures at the rootlet of the stereocilia, and the packed actin filaments (which impart the stereocilia with their rigidity) are depolymerized [20] [32]. Within the IHC tuft the damage to the tall, outer row of stereocilia is often selective; the shorter rows may remain ultrastructurally normal even when the tallest row is completely missing. Moreover, the tip links remain intact on the shorter stereocilia, suggesting that such IHCs may be capable of transduction, but with reduced sensitivity. Auditory-nerve fibers associated with such IHCs exhibit much lower rates of spontaneous activity [21]. Following acoustic overstimulation, tuning curves with elevated "tips" and "tails" are associated with significant decreases in mean spontaneous discharge rate, whereas tuning curves with elevated tips but hypersensitive tails are associated with a clear elevation of the mean spontaneous rates [21]. Our model, in which altered Brownian motion patterns of the stereocilia lead to changes in the spiking pattern, may help to account for the occurrence of such pathological spiking patterns. However, one should bear in mind that in hearing loss of cochlear origin there are other noise-induced changes, such as different steady-state Ca^{2+} concentrations, that are the result of altered Ca^{2+} pump kinetics. Such changes may also be responsible for the pathological spiking patterns.

Future studies of the coding efficiency of inner hair cells at the threshold of hearing should take into consideration the possibility that Brownian motion of the stereocilia changes along the tonotopic axis and may be tuned in such a way as to enhance the audibility of specific frequencies. Such studies should also carefully consider the potential significance of the adaptation process of mammalian-transduction-channel kinetics, as well as the stochastic-resonance phenomena that have recently been demonstrated in transduction channels [18] and in calcium-activated potassium channels in the basolateral IHC membrane (Jaramillo, personal communication).

Acknowledgements

References

[1] Ashmore, J. F. and Kolston, P. J. "Hair cell based amplification in the cochlea." *Curr. Opin. Neurobiol.*, 4: 503–8, 1994.

[2] Denk, W., Webb, W. W. and Hudspeth, A. J. "Mechanical properties of sensory hair bundles are reflected in their Brownian motion measured with a laser differential interferometer." *Proc. Nat. Acad. Sci.*, 16: 5371–5375, 1989.

[3] Derksen, H. E. "Axon membrane voltage fluctuations." *Act. Physiol. Pharmacol. Neerl.*, 13: 373–466, 1965.

[4] Derksen, H. E. and Verveen, A. A. "Fluctuations of resting neural membrane potential." *Science*, 151: 1388–1389, 1966.

[5] Ehrenberger, K. and Felix, D. "Glutamate receptors in afferent cochlear neurotransmission in guinea pigs." *Hear. Res.*, 52: 73–80, 1991.

[6] Felix, D. and Ehrenberger, K. "The efferent modulation of mammalian inner hair cell afferents." *Hear. Res.*, 64: 1–5, 1992.

[7] Felix, H., Gleeson, M. J., Pollak, A. and Johnsson, L. "The cochlear neurons in humans." *Progr. Hum. Audit. Vestib. Histopath.*, S. Iurano and J. E. Veldman (eds.), Amsterdam: Kugler, pp. 73–79, 1997.

[8] Gebeshuber, I. C., Mladenka, A., Rattay, F. and Svrcek-Seiler, W. A. "Computational demonstration that Brownian motion of inner hair cells stereocilia may enhance the ability to detect low level auditory tones from auditory nerve spiking patterns." *J. Physiol. (Lond.)*, 504P: 127P–128P, 1997.

[9] Gebeshuber, I. C., Mladenka, A., Rattay, F. and Svrcek-Seiler, W. A. "Brownian motion and the ability to detect weak auditory signals." In *Chaos and Noise in Biology and Medicine,* M. Barbi and S. Chillemi (Eds.), World Scientific: Singapore, pp. 230–237, 1999.

[10] Gebeshuber, I. C. "The influence of stochastic behavior on the human threshold of hearing." *Chaos, Solitons & Fractals*, 11: 1855–1868, 2000.

[11] Gebeshuber, I. C., Pontes Pinto, J., Naves Leao, R., Mladenka, A. and Rattay, F. "Stochastic resonance in the inner ear: the effects of endogenous transduction channel noise and stereociliary thermal motions on the human hearing threshold in various frequency bands." *ARGESIM Rep. 10: Proc. TU-BioMed Minisymp. 1998 "Brain Modelling"* F. Rattay (Ed.), pp. 40–44, 1998.

[12] Gleich, O., Narins, P. M. "The phase response of primary auditory afferents in a songbird (Sturnus vulgaris L.)." *Hear. Res.*, 32: 81–91,1988.

[13] Greenwood, D. D. "A cochlear frequency–position function for several species — 29 years later." *J. Acoust. Soc. Am.*, 87: 2592–2605, 1990.

[14] Hind, J. E. "Physiological correlates of auditory stimulus periodicity." *Audiology*, 11: 42–57, 1972.

[15] Hudspeth, A. J. "How the ear's works work." *Nature*, 341: 397–404, 1989.

[16] Hudspeth, A. J. "Mechanical amplification of stimuli by hair cells." *Curr. Opin. Neurobiol.*, 7: 480–486, 1997.

[17] Ivey, C., Apkarian, A. V. and Chialvo, D. R. "Noise-induced tuning curve changes in mechanoreceptors." *J. Neurophysiol.* 79: 1879–1890, 1998.

[18] Jaramillo, F. and Wiesenfeld, K. "Mechanoelectrical transduction assisted by Brownian motion: A role for noise in the auditory system." *Nature Neurosci.*, 1: 384–388, 1998.

[19] Javel, E. "Acoustic and electrical encoding of temporal information." In *Cochlear Implants — Models of the Electrically Stimulated Ear,* J. M. Miller and F. A. Spelman (eds.), New York: Springer–Verlag, pp. 247, 1990.

[20] Liberman, M. C. "Auditory-nerve response from cats raised in a low-noise chamber." *J. Acoust. Soc. Am.*, 63: 442–455, 1978.

[21] Liberman, M. C. and Dodds, L. W. "Single-neuron labeling and chronic cochlear pathology. II. Stereocilia damage and alterations of spontaneous discharge rates." *Hear. Res.*, 16: 43–53, 1984.

[22] Markin, V. S., Jaramillo, F. and Hudspeth, A. J. "The three-state model for transduction-channel gating in hair cells." *Biophys. J.*, 64: A93, 1993.

[23] McNamara, B. and Wiesenfeld, K. "The theory of stochastic resonance." *Phys. Rev. A*, 39: 4854–4869, 1989.

[24] Nobili, R., Mammano, F. and Ashmore, J. F. "How well do we understand the cochlea?" *Trends Neurosci.*, 21: 159–167, 1998.

[25] Rattay, F., Gebeshuber, I. C. and Gitter, A. H. "The mammalian auditory hair cell: A simple electric circuit model." *J. Acoust. Soc. Am.*, 103: 1558–1565, 1998.

[26] Rattay, F., Mladenka, A. and Pontes Pinto, J. "Classifying auditory nerve patterns with neural nets: A modeling study with low level signals." *Sim. Pract. Theor.*, 6: 493–503, 1998.

[27] Relkin, E. M. and Doucet, J. R. "Recovery from prior stimulation. I: Relationship to spontaneous firing rates of primary auditory neurons." *Hear. Res.*, 55: 215–222, 1991.

[28] Rose, J. E., Brugge, J. F., Anderson, D. J., Hind, J. E., "Phase-locked response to low-frequency tones in single auditory nerve fibers of the squirrel monkey." *J. Neurophysiol.*, 30: 769–793, 1967.

[29] Rose, J. E., Hind, J. E., Anderson, D. J., Brugge, J. F., "Some effects of stimulus intensity on response of auditory nerve fibers in the squirrel monkey." *J. Neurophysiol.*, 34: 685–699, 1971.

[30] Spoendlin, H. and Schrott, A. "Analysis of the human auditory nerve." *Hear. Res.*, 43: 25–38, 1989.

[31] Svrcek-Seiler, W. A., Gebeshuber, I. C., Rattay, F., Biró, T. and Markum, H. "Micromechanical models for the Brownian motion of hair cell stereocilia." *J. Theor. Biol.*, 193: 623–630, 1998.

[32] Tilney, L. G., Saunders, J. C., Egelman, E. and DeRosier, D. J. "Changes in the organization of actin filaments in the stereocilia of noise-damaged lizard cochleae." *Hear. Res.*, 7:181–197, 1982.

[33] Zwicker, E. *Psychoakustik*. Berlin: Springer–Verlag, p. 34, 1982.